ERDC Letter Report

Environmental Laboratory

US Army Corps of Engineers®
Engineer Research and Development Center

Modeling the Impact of Hurricane Ike and the October 1994 San Jacinto River Flood on the San Jacinto Waste Pits Cap

September 2017

Earl Hayter and Lihwa Lin

Lower San Jacinto River

9867570

The US Army Engineer Research and Development Center (ERDC) solves the nation's toughest engineering and environmental challenges. ERDC develops innovative solutions in civil and military engineering, geospatial sciences, water resources, and environmental sciences for the Army, the Department of Defense, civilian agencies, and our nation's public good. Find out more at www.erdc.usace.army.mil.

To search for other technical reports published by ERDC, visit the ERDC online library at http://acwc.sdp.sirsi.net/client/default.

Modeling the Impact of Hurricane Ike and the October 1994 San Jacinto River Flood on the San Jacinto Waste Pits Cap

Earl Hayter

Environmental Laboratory
U.S. Army Engineer Research and Development Center
3909 Halls Ferry Road
Vicksburg, MS 39180-6199

Lihwa Lin

Coastal and Hydraulics Laboratory
U.S. Army Engineer Research and Development Center
3909 Halls Ferry Road
Vicksburg, MS 39180-6199

Letter Report

Approved for public release; distribution is unlimited.

Prepared for U.S. EPA, Region 6
Dallas, TX 75202

Abstract

The U.S. Army Engineer Research and Development Center (ERDC) is providing technical support to the US Environmental Protection Agency (EPA), the goal of which is to evaluate the potential impact of Hurricane Ike and the October 1994 San Jacinto River Flood on the San Jacinto Waste Pits Cap for the San Jacinto River Waste Pits Superfund Site, Texas. The specific objectives of this study are the following:

- Model the simultaneous occurrence of Hurricane Ike and the October 1994 San Jacinto River flood on the San Jacinto Waste Pits cap to determine the maximum current- and wave-induced bed shear stresses that the proposed alternative 3aN cap would be subjected to.

- Using those maximum bed shear stresses, estimate the potential (but not the depth of erosion since sediment transport modeling was not performed) for erosion of the proposed alternative 3aN cap.

This report presents the results from this task that was identified by EPA for ERDC to perform. The results of the modeling showed that some erosion of the alternative 3aN cap would occur in all four quadrants (i.e., SE, SW, NE, NW) of the cap during this hypothetical storm event. The depth of maximum erosion cannot be determined since sediment transport modeling was not performed.

Contents

Abstract ii

Preface v

Unit Conversion Factors vi

Summary and Conclusions 1

1 Introduction 2
- Background 2
- Goal and Objectives 4

2 Site Description 5
- Hydrology and Hydrodynamics of the San Jacinto River 5

3 Hydrodynamic Modeling 7
- Model Setup 7
  - Boundary Conditions 7
  - Model Calibration 8
- Model Results 10

4 Wave Modeling 14
- Model Setup 14
  - Boundary Conditions 15
- Model Results 17

5 Evaluation of Alternative 3aN Cap Stability 22
- Methodology 22

References 25

Appendix A: Description of Modeling System 28

Appendix B: Description of Hydrodynamic Module 30

Figures and Tables

Figures

Figure 1-1 San Jacinto River Waste Pits Superfund Site. 3
Figure 3-1 Expanded LTFATE Model Domain used to simulate Hurricane Ike. 8
Figure 3-2 Measured tides at the entrance to Galveston Bay. 9
Figure 3-3 Measured discharge applied at the upstream boundary in the San Jacinto River. 10
Figure 3-4 Four grid cells that represent the San Jacinto River Waste Pits cap 11
Figure 3-5 Simulated water depths at the San Jacinto River Waste Pits cap 11
Figure 3-6 Simulated average water surface elevation at the San Jacinto River Waste Pits cap 12
Figure 3-7 Simulated velocities in the SE quadrant of the San Jacinto River Waste Pits cap 13
Figure 4-1 Location map of Galveston Bay system 16
Figure 4-2 CMS-Wave model domain and depth contours 17
Figure 4-3 Available wind and wave data in September 2008 18
Figure 4-4 Water level measurements in September 2008 19
Figure 4-5 Model calculated wave field at 0100 GMT, 15th August, 2008 20
Figure 4-6 Model calculated wave field at 0400 GMT, 13th September, 2008 20
Figure 4-7 Simulated wave heights and periods in the SE quadrant of the San Jacinto River Waste Pits cap 21
Figure 5-1 Calculated current- and wave-induced bed shear stress at the SE quadrant of the San Jacinto Waste Pits cap 23
Figure 5-2 Calculated current- and wave-induced bed shear stress in all four quadrants of the San Jacinto Waste Pits cap 24

Preface

This study was performed at the request of the U.S. Environmental Protection Agency (EPA) – Region 6 by the Environmental Laboratory (ERDC-EL) of the US Army Corps Engineer Research and Development Center (ERDC), Vicksburg, MS.

At the time of publication, the Deputy Director of ERDC-EL was Dr. Jack E. Davis and the Director of ERDC-EL was Dr. Elizabeth C. Fleming. Commander of ERDC was COL Bryan S. Green. The Director was Dr. David W. Pittman.

Unit Conversion Factors

Multiply	By	To Obtain
Feet	0.3048	meters
miles (U.S. nautical)	1,.852	kilometers
miles (U.S. statute)	1.609347	kilometers
Acres	4,046.873	Square meters
cubic yards	0.7645549	cubic meters
Knots	0.5144444	Meters per second

Summary and Conclusions

The U.S. Army Engineer Research and Development Center (ERDC) is providing technical support to the US Environmental Protection Agency (EPA), the goal of which is to evaluate the potential impact of Hurricane Ike and the October 1994 San Jacinto River Flood on the San Jacinto Waste Pits Cap for the San Jacinto River Waste Pits Superfund Site, Texas. The specific objectives of this study are the following:

- Model the simultaneous occurrence of Hurricane Ike and the October 1994 San Jacinto River flood on the San Jacinto Waste Pits cap to determine the maximum current- and wave-induced bed shear stresses that the proposed alternative 3aN cap would be subjected to.

- Using those maximum bed shear stresses, estimate the potential (but not the depth of erosion since sediment transport modeling was not performed) for erosion of the proposed alternative 3aN cap.

This report presents the results from this task that was identified by EPA for ERDC to perform. The results of the modeling showed that some erosion of the alternative 3aN cap would most likely occur over most of the cap during this hypothetical storm event. Specifically, some erosion would be expected to occur in all four quadrants (i.e., SE, SW, NE, NW) of the cap. The depth of maximum erosion in each of the four quadrants cannot be determined from this analysis since sediment transport modeling was not performed.

DRAFT

1 Introduction

Background

The San Jacinto River Waste Pits Superfund Site (Site) consists of several waste ponds, or impoundments, approximately 14 acres in size, built in the mid-1960s for the disposal of paper mill wastes as well as the surrounding areas containing sediments and soils potentially contaminated by the waste materials that had been disposed of in these impoundments. The impoundments are located immediately north and south of the I-10 Bridge and on the western bank of the San Jacinto River in Harris County, Texas (see Figure 1-1).

Large scale groundwater extraction has resulted in regional subsidence of land in proximity to the Site that has caused the exposure of the contents of the northern impoundments to surface waters. A time-critical removal action was completed in 2011 to stabilize the pulp waste material in the northern impoundments and the sediments within the impoundments to prevent further release of dioxins, furans, and other chemicals of concern into the environment. The removal consisted of placement of a temporary armor rock cap over a geotextile bedding layer and an impermeable geomembrane in some areas. The total area of the temporary armor cap is 15.7 acres. The cap was designed to withstand a 100-year storm event.

The southern impoundments are located south of I-10 and west of Market Street, where various marine and shipping companies have operations (see Figure 1-1). The area around the former southern impoundments is an upland area that is not currently in contact with surface water.

The first author of this ERDC Letter Report have provided technical assistance to the Site's Remedial Project Manager (RPM) for the past five years that consisted of an evaluation of modeling performed by the modeling contractor for the Potentially Responsible Parties (PRP).

DRAFT

Figure 1-1 San Jacinto River Waste Pits Superfund Site

Goal and Objectives

The goal of this study is to provide technical support to US Environmental Protection Agency (EPA), specifically to evaluate the potential impact of Hurricane Ike and the October 1994 San Jacinto River Flood on the San Jacinto Waste Pits Cap for the San Jacinto River Waste Pits Superfund Site, Texas. The specific objectives of this study are the following:

- Model the simultaneous occurrence of Hurricane Ike and the October 1994 San Jacinto River flood on the San Jacinto Waste Pits cap to determine the time series of current- and wave-induced bed shear stresses that the proposed alternative 3aN cap would be subjected to.

- Using the simulated current- and wave-induced bed shear stresses, estimate the potential (but not the depth of erosion since sediment transport modeling was not performed) for erosion of the proposed alternative 3aN cap.

This report presents the results from this task that was identified by EPA for ERDC to perform.

DRAFT

2 Site Description

Hydrology and Hydrodynamics of the San Jacinto River

The lower San Jacinto River (SJR) is classified as a coastal plain estuary. Dyer (1997) gives the following definition of an estuary: "An estuary is a semi-enclosed coastal body of water which has a free connection to the open sea, extending into the river as far as the limit of tidal influence, and within which sea water is measurably diluted with fresh water derived from land drainage." Land drainage is from the SJR watershed which is a 4,500 square mile area in Harris County, TX. Bedient (2013) reports that this watershed drains an average of approximately two million acre-feet (2.47 km^3) of runoff per year. The SJR connects to Galveston Bay which has open connections to the Gulf of Mexico.

The SJR Waste Pits are located in a FEMA designated floodway zone, which is essentially the 100-year floodplain for the SJR. The base flood elevation, which is the water surface elevation resulting from a 100-year flood, for the waste pits has been determined by FEMA to be 19 feet (5.8 m). The low lying Waste Pits are also subject to flooding from storm surges generated by both tropical storms (*i.e.*, hurricanes) and extra-tropical storms. Storm surges generated in the Gulf of Mexico propagate into Galveston Bay and into the Lower SJR. Storm surge modeling conducted by NOAA predicted that category 3 and 5 hurricanes that hit Galveston Bay during high tide would produce surge levels of 23 ft (7.0 m) and 33 ft (10.1 m), respectively, at the Site. In addition, eustatic sea level rise and subsidence also contributes to the vulnerability of the Site. The combined effect of sea level rise and subsidence is reflected in the 1.97 ft (0.6 m) increase in relative sea level rise recorded over the past 100 years in Galveston Bay (Brody *et al.* 2014).

The dynamic nature of the flow regime in the SJR estuary is exemplified by the flood that occurred from October 15-19, 1994. The flood was caused by rainfall that ranged from 8 to more than 28 inches during this five-day period and caused severe flooding in portions of 38 counties in southeast Texas (USGS 1995). The 100-year flood was equaled at three of the 43

DRAFT

streamflow gauging stations in the 29 counties that were declared disaster areas after the flow, and it was exceeded at 16 stations. The exceedance of the 100-year flood at the 16 stations ranged from a factor of 1.1 to 2.9 times the 100-year flood. In addition, at 25 of the 43 stations, the peak stages during the flood exceeded the historical maximums (USGS 1995). This flood had a 360,000 ft^3/s (cfs) (10,194 m^3/s (cms)) peak streamflow, 27.0 ft (8.2 m) peak stage, and current velocities greater than 15 ft/s (4.6 m/s) at the USGS gage station No. 08072050 on the SJR near Sheldon, TX when up to eight feet of scour was reported in the reach of the SJR south of the I-10 Bridge. However, no official documentation of this amount of scour was found during our extensive literature search. The photo on the report front cover shows the inundated Site during this flood.

As another example, Hurricane Ike, which was a category 2 hurricane, hit Galveston Bay on September 15, 2008. While this hurricane was less than a 100-year storm, it produced a large storm surge that completely inundated the Site and generated a peak flow rate of 63,100 cfs (1,787 cms) at the Lake Houston Dam. The peak stage at the USGS Station No. 08072050 during Hurricane Ike was 14.2 ft (4.33 m). Tropical Storm Allison hit the Galveston Bay area on June 10, 2001, and generated a peak flow rate at the Lake Houston Dam of 80,500 cfs (2,280 cms). USGS Station No. 08072050 was not installed until October 1, 2007, so the peak stage during Allison is not known.

DRAFT

3 Hydrodynamic Modeling

Model Setup

For simulating the impact of Hurricane Ike on the SJR Site, the model domain for LTFATE had to be expanded to include Galveston Bay to be able to simulate the propagation of the storm surge into the SJR estuary. The expanded model domain is shown in Figure 3-1. A Cartesian grid with 131,989 120m by 120m size grid cells was constructed. The grid had to be coarsened from the initial San Jacinto River model due to the larger number of grid cells in the expanded model domain that greatly lengthened the model run times. The time period simulated was June – September 2008. The first 2.0 months of these four months was used to spin-up the hydrodynamic model, with the latter hot-started to simulate August – September 2008 that included Hurricane Ike. Wave modeling was performed, using a one-hour time step, for the 1.5 month period between August 15 – September 30 2008 using the CMS-Wave model. This modeling is described below. The time series of simulated wave heights, periods and directions were read during the LTFATE model run and used to calculate the current- and wave-induced bed shear stresses.

As stated previously, the simulation of Hurricane Ike also included the hypothetical synoptic occurrence of the October 1994 San Jacinto River flood on the San Jacinto Waste Pits cap to determine the time series of current- and wave-induced bed shear stresses that the proposed alternative 3aN cap would be subjected to under this extreme scenario. For this hypothetical scenario, the timing of the October 1994 flood, which had a peak discharge of approximately 11,000 cms (390,000 cfs), was adjusted to occur at the time of the peak storm surge height at the Site. Due to the lack of salinity data over the water depth at the downstream boundary, the LFATE model was run in a two-dimensional, depth-averaged model like AQ's model.

Boundary Conditions

The same simulated freshwater flows from the bayous along the Houston ship channel used by Anchor QEA (AQ) in their hydrodynamic model for the period June 1 – September 30, 2008 were also included in the LTFATE simulation. The measured water surface elevations at the

DRAFT

entrance to Galveston Bay was used as the tidal forcing (see Figure 3-2).

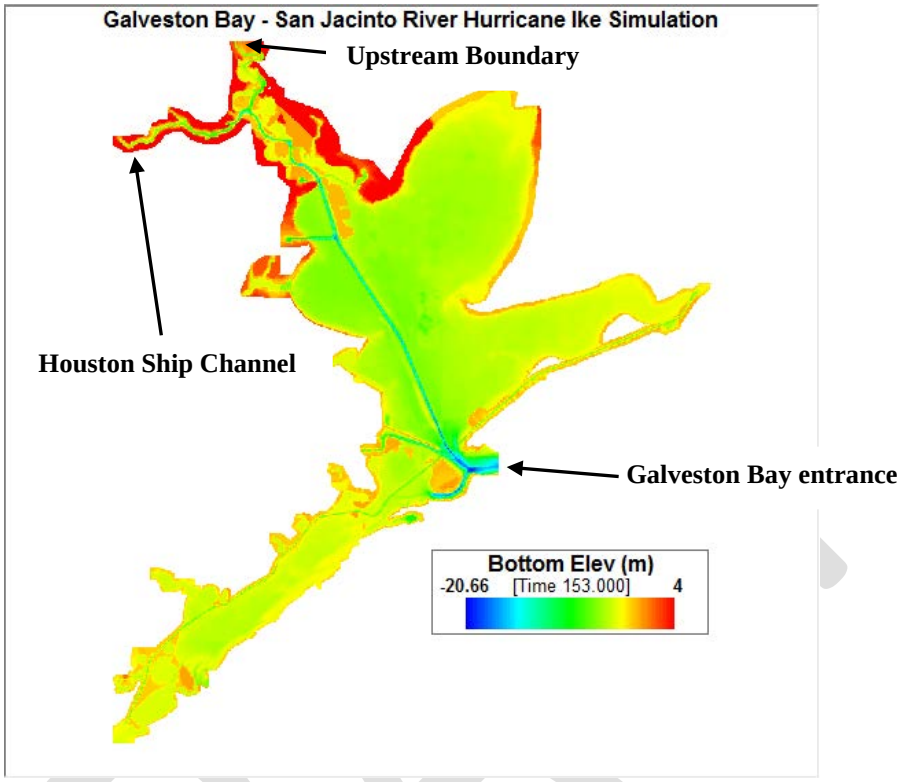

Figure 3-1 Expanded LTFATE Model Domain used to simulate Hurricane Ike

Day 152 to Day 213 was the hydrodynamic spin-up period, and Day 214 to Day 275 was the hot-started simulation period for which the current- and wave-induced bed shear stresses at the San Jacinto River Waste Pits cap were calculated. Day 260 (September 13, 2008) was the time when the water surface elevation at the entrance to Galveston Bay was maximum during Hurricane Ike. Figure 3-3 shows the measured discharge that was applied at the upstream boundary of the San Jacinto River (see Figure 3-1).

Model Calibration

The same data sets used to calibrate the AQ hydrodynamic model (ADCP surveys conducted June 13 – July 7, 2010 and May 10 – July 13, 2011) were used to calibrate LTFATE. The optimum agreement in the simulated and measured water levels and depth-averaged velocities was achieved

using a globally averaged value of 0.1 cm for z_o = effective bed roughness that represents to total bottom roughness due to both skin friction and form drag. The root-mean-square error (RMSE), which represents the standard deviation of the model error, in the water surface elevations for the 2010 and 2011 periods were 5.13 cm and 5.29 cm, respectively. The RMSE error in the depth-averaged velocities for the 2010 and 2011 periods were 0.18 m/s and 0.24 m/s, respectively. These results were deemed satisfactory to perform the modeling study described herein.

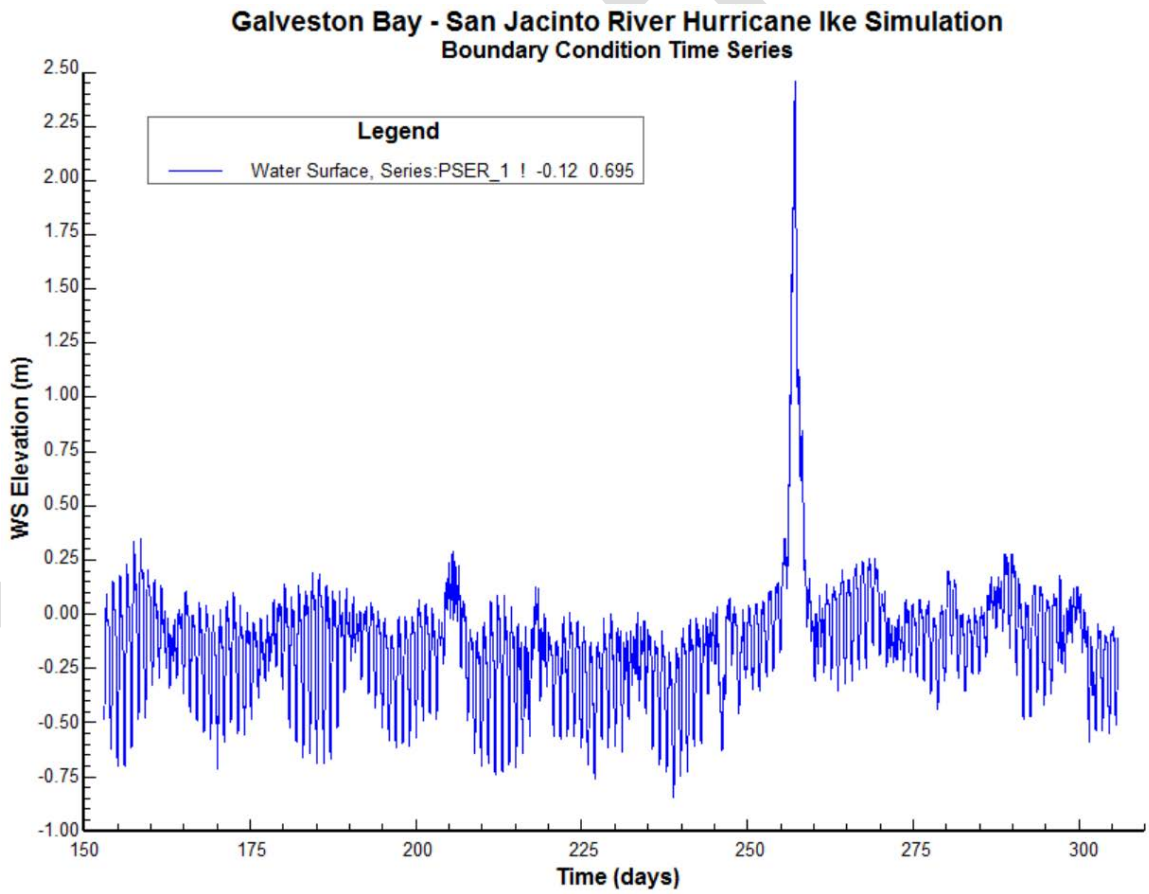

Figure 3-2 Measured tides at the entrance to Galveston Bay

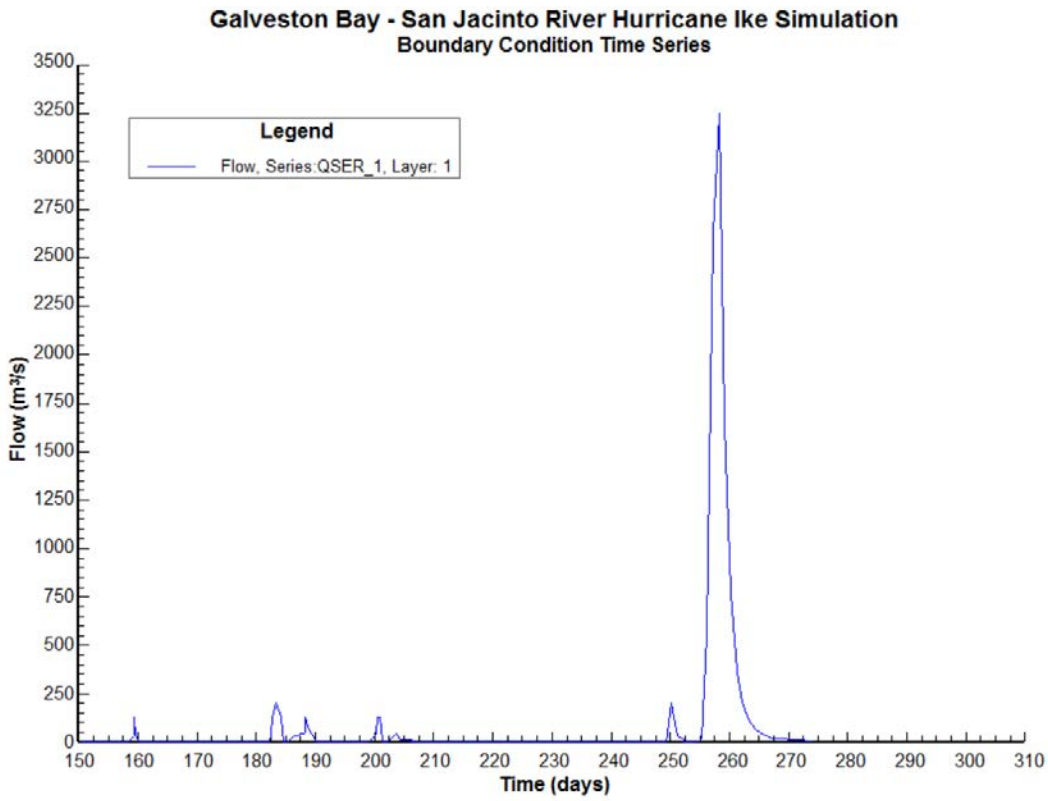

Figure 3-3 Measured discharge applied at the upstream boundary in the San Jacinto River

Model Results

The coarser grid used in this simulation resulted in four grid cells covering the cap. Figure 3-4 shows the four grid cells. Figure 3-5 shows the simulated water depths at all four cells. The four cells shown in the legend are located (from top to bottom) in the SW, NW, NE, and SE quadrants of the cap. The Hurricane Ike storm surge as well as the higher elevation from the October 1994 record flood in the San Jacinto River results in large water depths around the peak of the two extreme events, i.e., Day 260. The average water surface elevation time series in the four cells is shown in Figure 3-6. As an example, Figure 3-7 shows the simulated velocities at the SE quadrant of the cap.

The hydrodynamics

Figure 3-4 Four grid cells that represent the San Jacinto Waste Pits cap

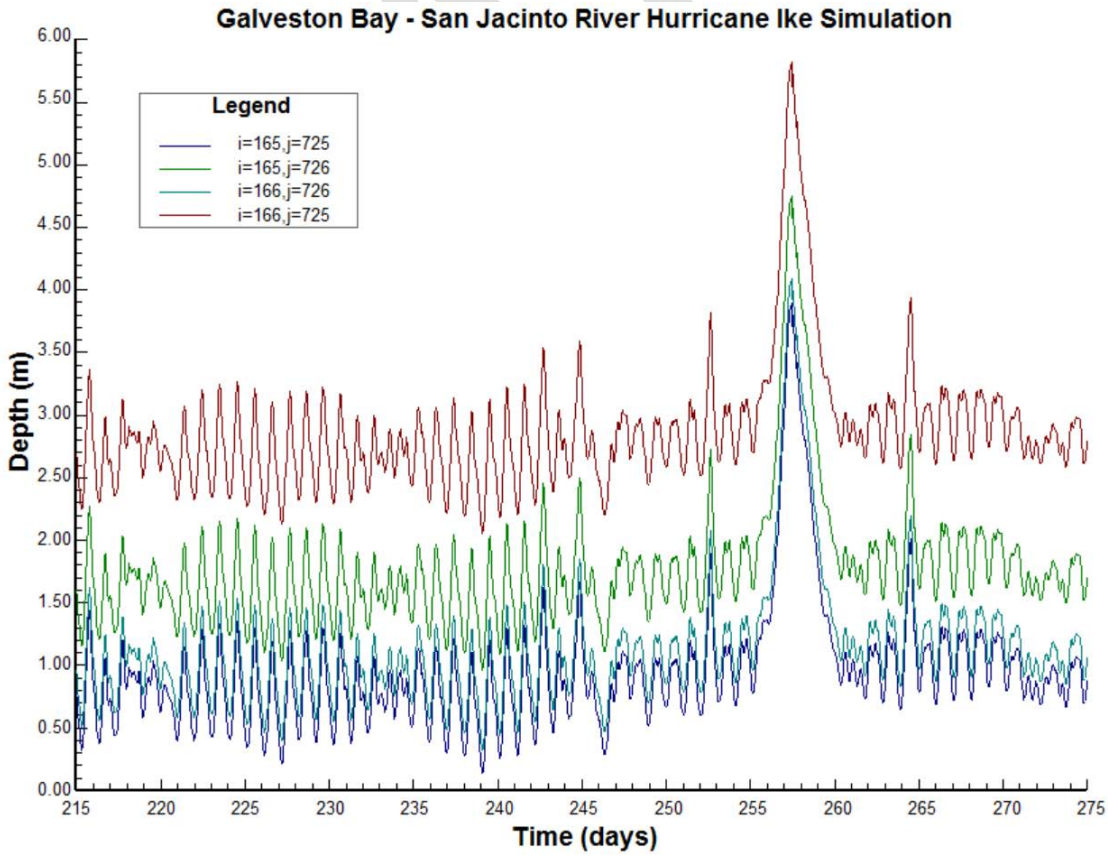

Figure 3-5 Simulated water depths at the San Jacinto River Waste Pits cap

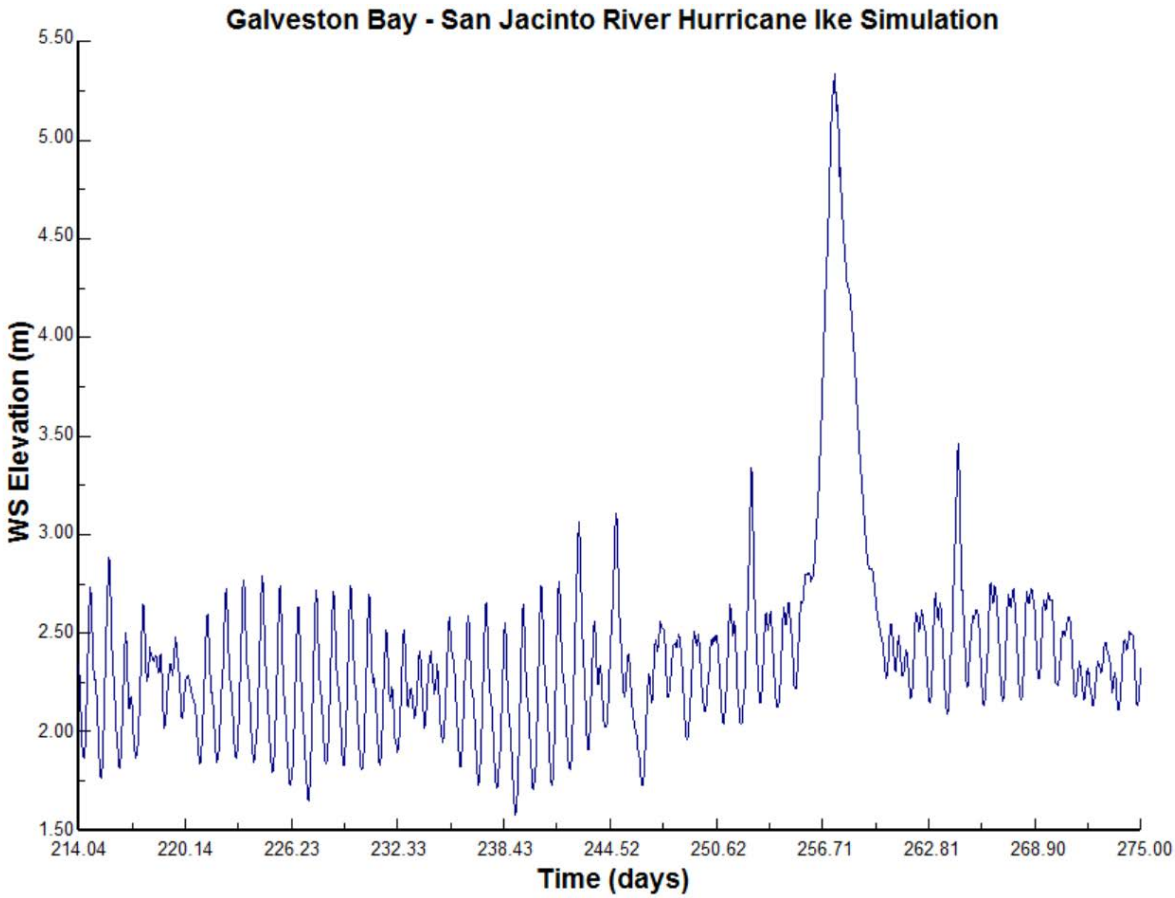

Figure 3-6 Simulated average water surface elevation at the San Jacinto River Waste Pits cap

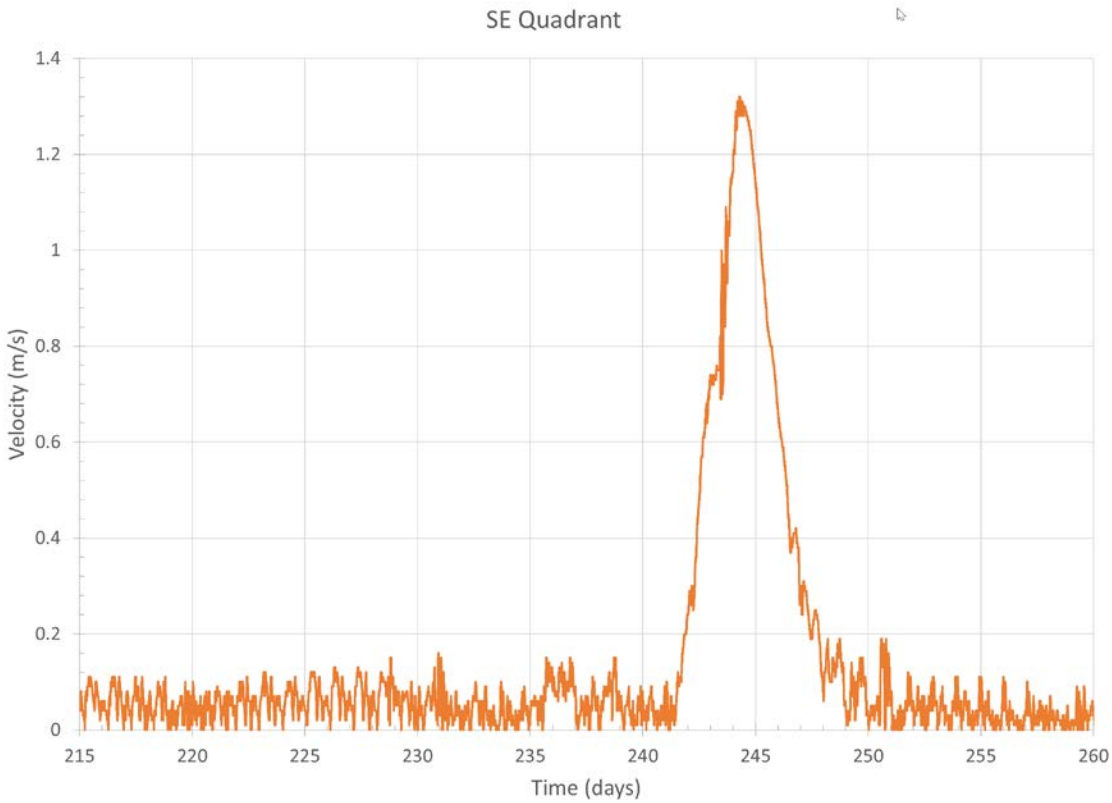

Figure 3-7 Simulated velocities in the SE quadrant of the San Jacinto River Waste Pits cap

DRAFT

4 Wave Modeling

Model Setup

The purpose of the numerical wave modeling is to estimate storm waves during Hurricane Ike at the northern Galveston Bay and Port of Houston. Wave modeling was conducted using CMS-Wave, a steady-state two-dimensional spectral wave model (Lin *et al.* 2008; Lin *et al.* 2011a, 2011b) capable of simulating wind waves in the open coast or in a bay or estuarine system. CMS-Wave is part of an integrated Coastal Modeling System (Demirbilek and Rosati 2011) developed at CHL to assist in coastal region project applications.

CMS-Wave can be used either in half-plane or full-plane mode for wind wave generation and transformation. It is based on the wave-action balance equation that includes wave propagation, refraction, shoaling, diffraction, reflection, breaking, and dissipation. The half-plane mode is the default and CMS-Wave can run more efficiently in this mode as waves are transformed primarily from the seaward boundary toward shore.

In the present study, CMS-Wave full-plane mode was used to simulate storm wave conditions during Hurricane Ike at the northern Galveston Bay and Port of Houston. The CMS-Wave uses the Surface-water Modeling System, SMS (Demirbilek *et al.* 2007; Zundel 2006) interface for grid generation, model setup, and post-processing.

Bay bathymetry data available for the wave modeling included LiDAR (http://shoals.sam.usace.army.mil) and periodic channel surveys conducted by the USACE Galveston District. The offshore bathymetry data were obtained from the US Coastal Relief Model by National Geophysical Data Center, NGDC (http://www.ngdc.noaa.gov/mgg/coastal/crm.html). The upland topography was downloaded from NOAA Gridded Global Topography Database (http://www.ngdc.noaa.gov/mgg/topo/topo.html). The digital coastlines are available from GEOphysical DAta System GEODAS (https://www.ngdc.noaa.gov/mgg/geodas/geodas.html).

The CMS model domain covers the Galveston Bay system with navigation channels connecting GIWW, Port of Houston, and Gulf of Mexico. It

DRAFT

includes the Houston-Galveston Ship Channel, Galveston Entrance Channel between the east end of Galveston Island and the west end of Bolivar Peninsula, San Luis Pass between the west end of Galveston Island and the east end of Follets Island, and Rollover Pass, a small man-made cut located at the lower east end of East Bay. Figure 4-1 shows the Galveston Bay system included in the present wave modeling area.

The CMS model grid extends approximately 60 mi (95 km) alongshore and 54 mi (86 km) cross-shore with the southern offshore boundary reaching to the 60-ft (18-m) isobaths, referenced to Mean Sea Level (MSL). Figure 4-2 shows the model domain consisting of 1166 × 1406 cells with variable cell spacing of 130 ft (40 m) along the Houston-Galveston Ship Channel and 660 ft (200 m) at the corners of offshore boundary.

Boundary Conditions

Wind and water level data used to force the wave model are available from three NOAA coastal stations (http://tidesandcurrents.noaa.gov): Sta 8771013 at Eagle Point (29° 28' 54" N, 94° 55' 0" W), Sta 8770613 at Morgans Point (29° 40' 54" N, 94° 59' 6" W), and Sta 8771341 at Galveston Bay entrance north jetty (29° 21' 24" N, 94° 43' 30" W). Directional wave spectra measured from NDBC Buoy 42035 (29° 13' 54" N, 94° 24' 46" W) offshore Galveston Bay Entrance (Figure 4-2) are use as incident waves along the wave model Gulf boundary. Buoy 42035 also collects surface wind data. Figure 4-3 shows the hourly wind and wave data measured from NOAA Stations 8771013, 8770613, 8771341, and NDBC Buoy 42035 in September 2008. Strong winds with large waves observed around September 13 are corresponding to Hurricane Ike during landfall near the Galveston Bay entrance. Figure 4-4 shows the water level data collected at three NOAA coastal stations in September 2008. High water levels occurred on September 13 corresponding to the storm surge during Hurricane Ike.

DRAFT

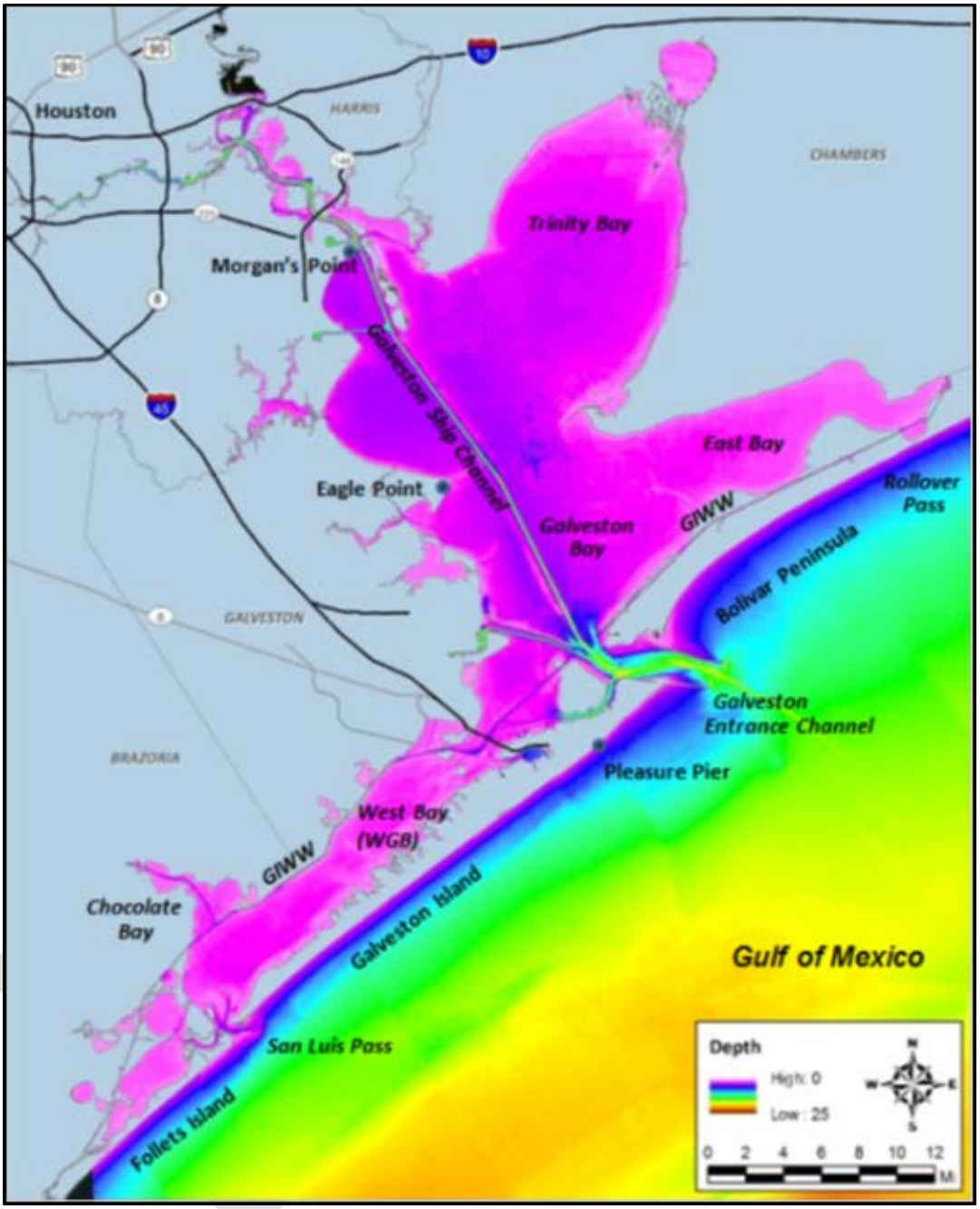

Figure 4-1. Location map of Galveston Bay system

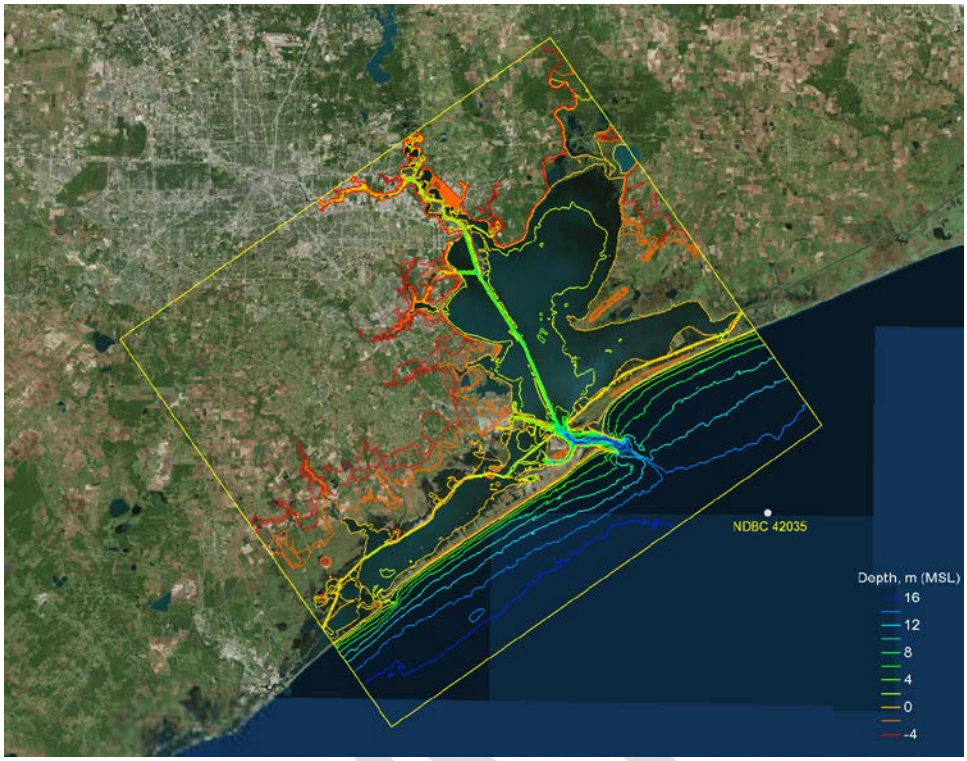

Figure 4-2. CMS-Wave model domain and depth contours

Model Results

Wave simulation was conducted for Hurricane Ike for period of 15 August to 30 September 2008 with the wind, water level, and incident wave input in 1-hr interval. The wind and incident wave input was based on Buoy 42035 data. The water level input was based on NOAA Sta 8771013 at Eagle Point. Wave runup and wave setup calculations were included in the model simulation. Figure 4-5, as an example, shows the model wave field under pre-Ike condition (incident wave height = 0.60 m, mean period = 6.2 sec, water level = 0 m, MSL, and wind speed = 6.7 m/sec from SSE) at 0100 GMT, 15th August 2008. Maximum wave height along the north perimeter of Galveston Bay is 0.28 m (mean period = 2.3 sec). Figure 4-6 shows the storm wave field under high water level during Ike inside Galveston Bay (incident wave height = 5.3 m, mean period = 14.3 sec, water level = 2.5 m, MSL, and wind speed = 30.0 m/sec from SE) at 0400 GMT, 13th September 2008. Maximum wave height inside the bay is 1.4 m (mean period = 4.0 sec). Model results clearly show larger waves under strong wind and over high water level during Ike along the northern

perimeter of Galveston Bay and around the Port of Houston area. As an example, Figure 4-7 shows the simulated wave heights and periods at the SE quadrant of the cap.

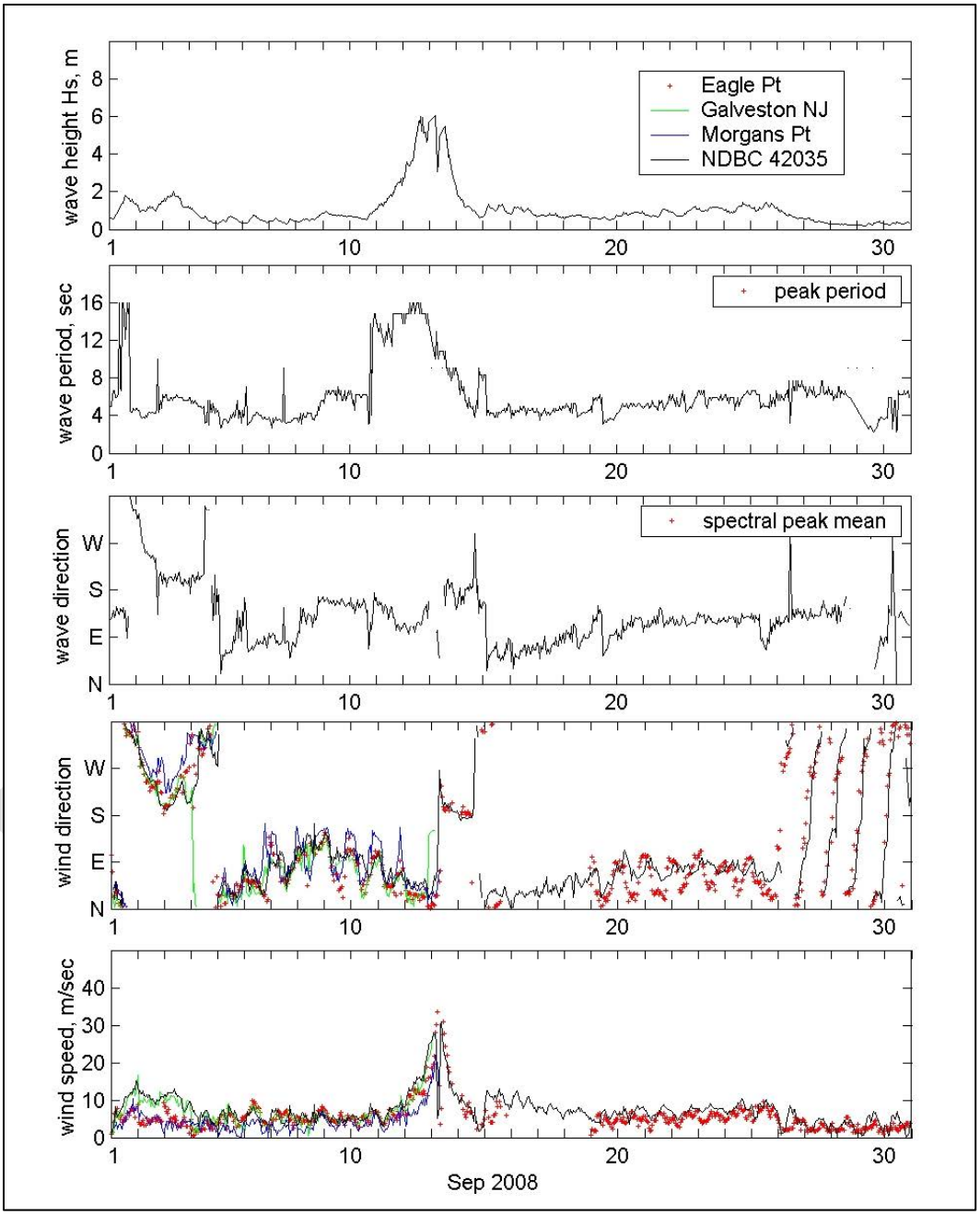

Figure 4-3. Available wind and wave data in September 2008

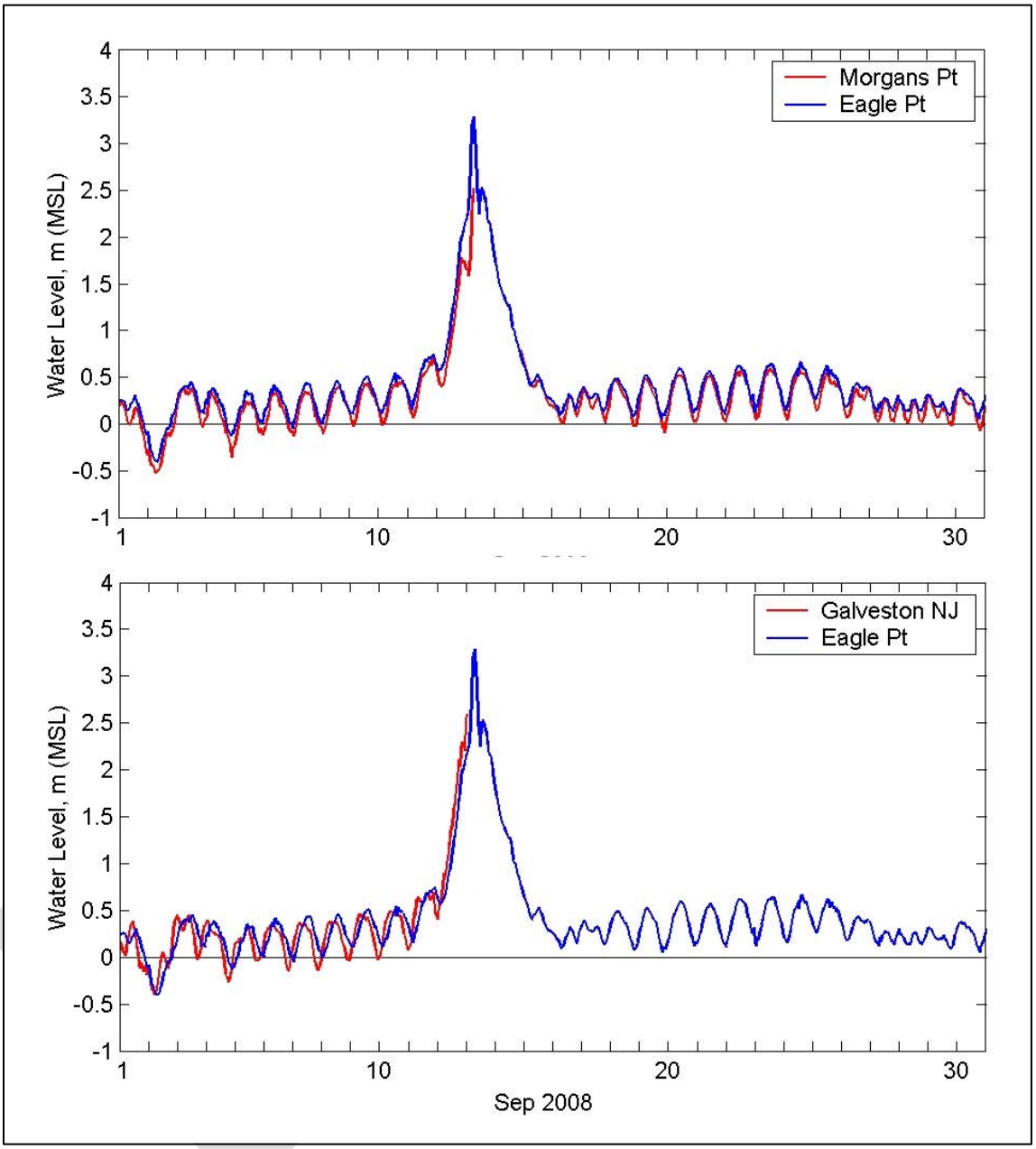

Figure 4-4. Water level measurements in September 2008

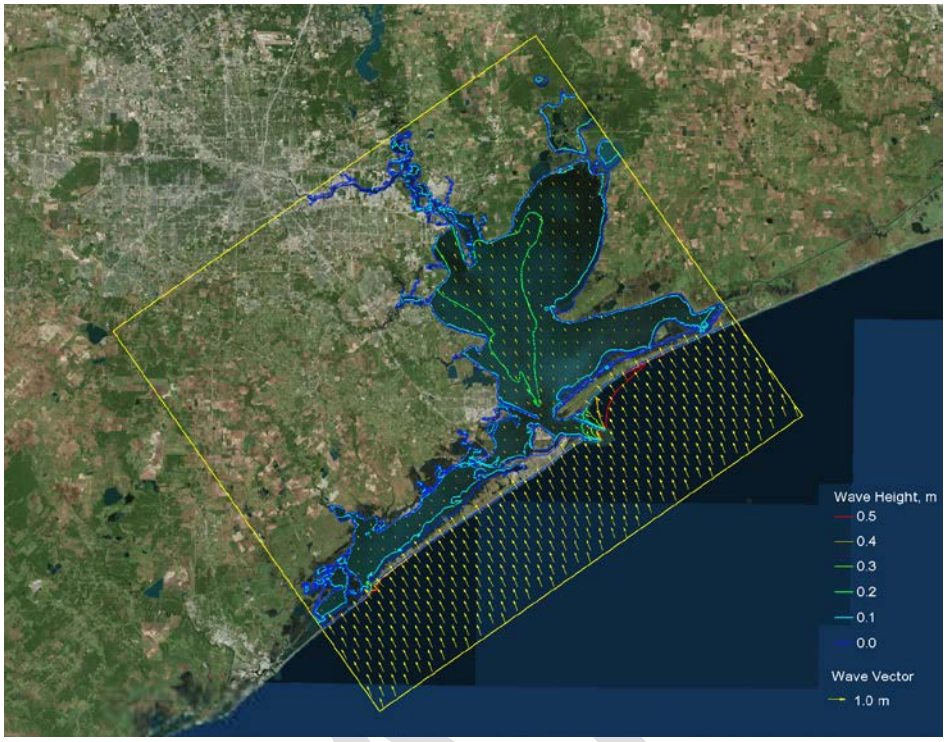

Figure 4-5. Model calculated wave field at 0100 GMT, August 15, 2008

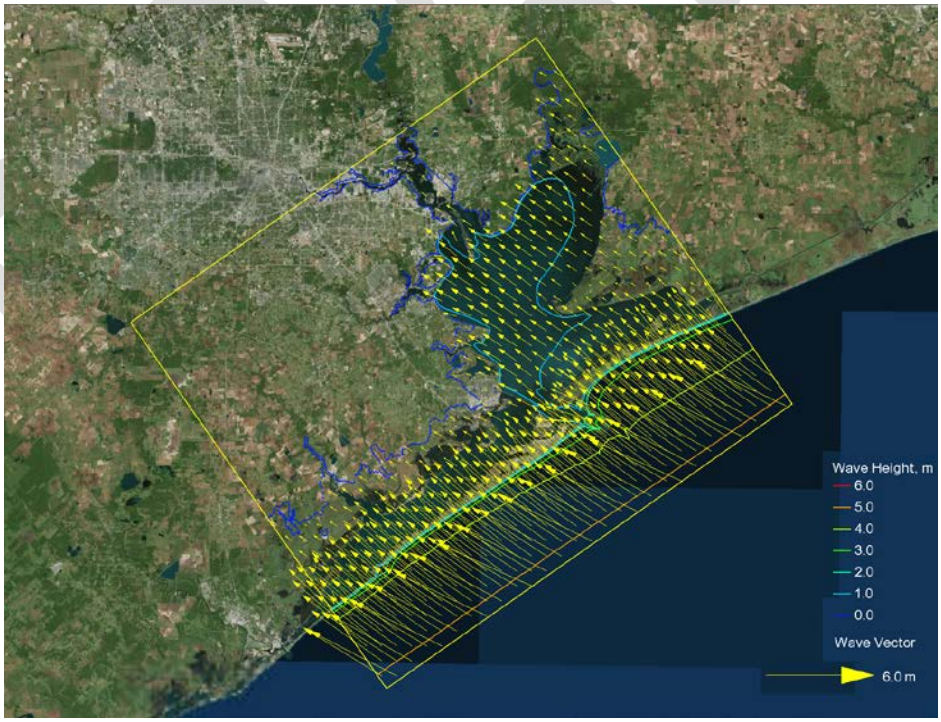

Figure 4-6. Model calculated wave field at 0400 GMT, September 13, 2008

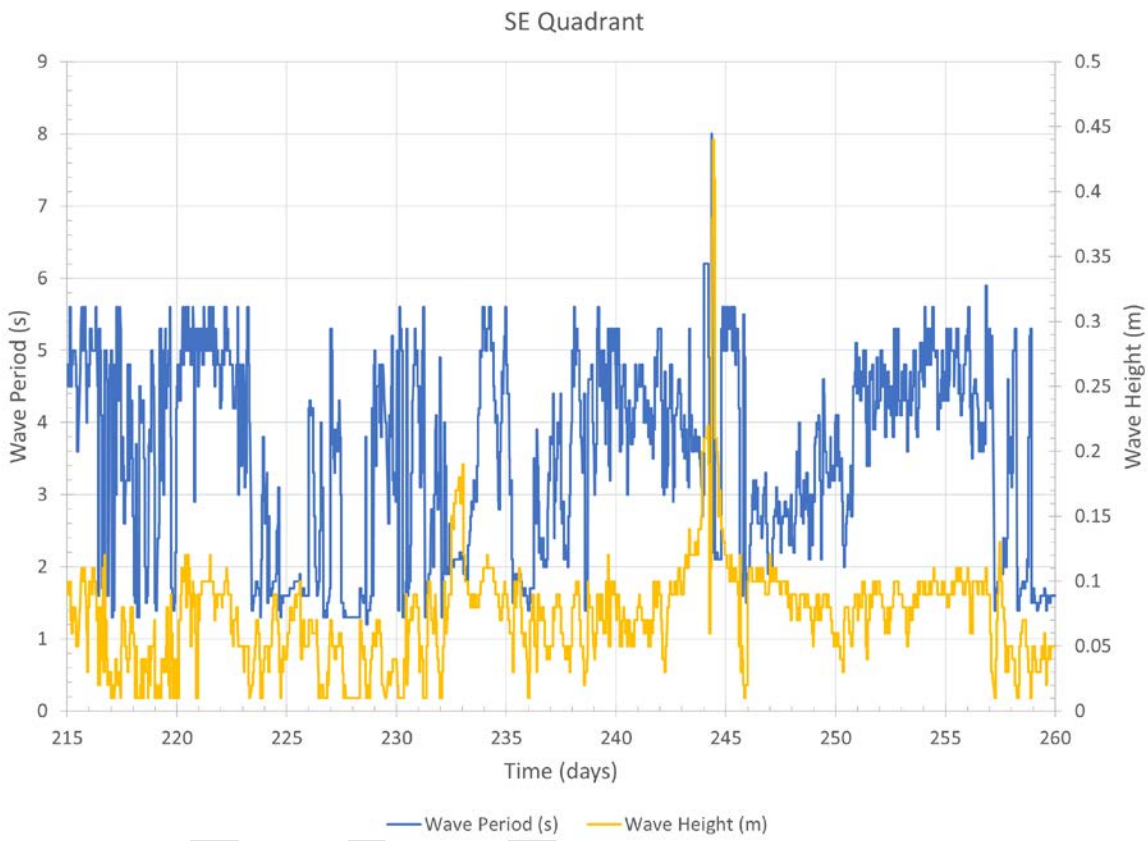

Figure 4-7. Simulated wave heights and periods at the SE quadrant of the San Jacinto Waste Pits cap

5 Evaluation of Alternative 3aN Cap Stability

Methodology

The four grid cells that represent the San Jacinto Waste Pits site (Figure 3-4) were modified to represent the proposed alternative 3aN cap. For the purpose of this hydrodynamic and wave modeling study, the bed roughness in those four cells was set to the recommended D_{50} value of 16.24 cm (6.4 inches). The current- and wave-induced bed shear stresses in these four grid cells were calculated to evaluate the potential for erosion of the caps during the hypothetic combined Hurricane Ike and October 1994 San Jacinto River flood. Note that the wave contribution to the total bed shear stress is an average of 10 percent of the total bed shear stress at these four grid cells. As an example, Figure 5-1 shows the calculated bed shear stress at the SE quadrant grid cell. The two dashed horizontal lines show the incipient critical bed shear stress, 144 Pa, and the suspension critical shear stress, 467 Pa, for sediment with a diameter of 16.24 cm. This figure shows that only the incipient critical shear stress was exceeded for a very short time in the SE quadrant of the alternative 3aN cap. This means that the armor at the surface of the cap could be moved as bedload but not in suspension, and as such, some erosion would be expected to occur in this section of the alternative 3aN cap.

Figure 5-2 shows the bed shear stress at all four grid cells that represent the alternative 3aN cap. This figure is zoomed in to the three days (Days 243 – 246) when the simulated storm was at its peak at the site. As seen, there is a period of time when even the suspension critical shear stress is exceeded in the SW quadrant of the site. As such, more erosion would be expected to occur in this quadrant of the alternative 3aN cap than in the other three quadrants. However, without performing sediment transport modeling, it is not possible to estimate the depth of maximum erosion that would occur.

Some erosion would also be expected to occur in both the NE and NW quadrants since the maximum bed shear stresses exceed the incipient critical bed shear stress of 144 Pa. Since the time intervals during which the bed shear stress exceeds the incipient shear stress are greater in both

the NE and NW quadrants than in the SE quadrant, qualitatively more erosion would be expected to occur in the NE and NW quadrants than in the SE quadrant.

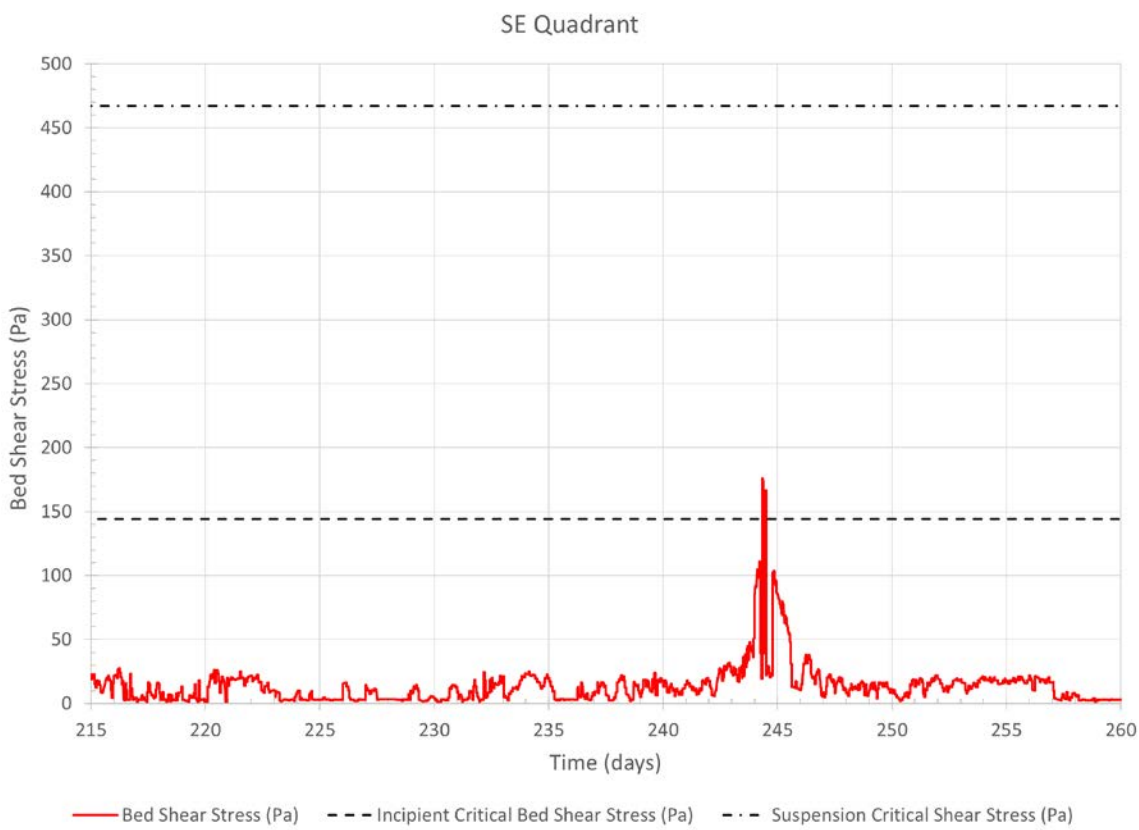

Figure 5-1 Calculated current- and wave-induced bed shear stress at the SE quadrant of the San Jacinto Waste Pits cap

These results should not be used to compare to the results of any other simulation than the sediment transport simulation performed by Hayter *et al.* (2016) of the same combined hypothetic event, i.e., simultaneous occurrence of Hurricane Ike and the October 1994 flood. Because of the vastly different hydrodynamics, it is not possible to compare results from only a riverine flood (e.g., October 1994 flood) to that during the hypothetical combination of a hurricane induced storm surge and a riverine flood. It also needs to be emphasized that the bed shear stresses at the cap during these two simulated events are not identical due to the

different size armor material used in the two simulated armored caps. Specifically, the bed shear stresses for the alternative 3aN cap are larger because of the use of larger armor in this cap.

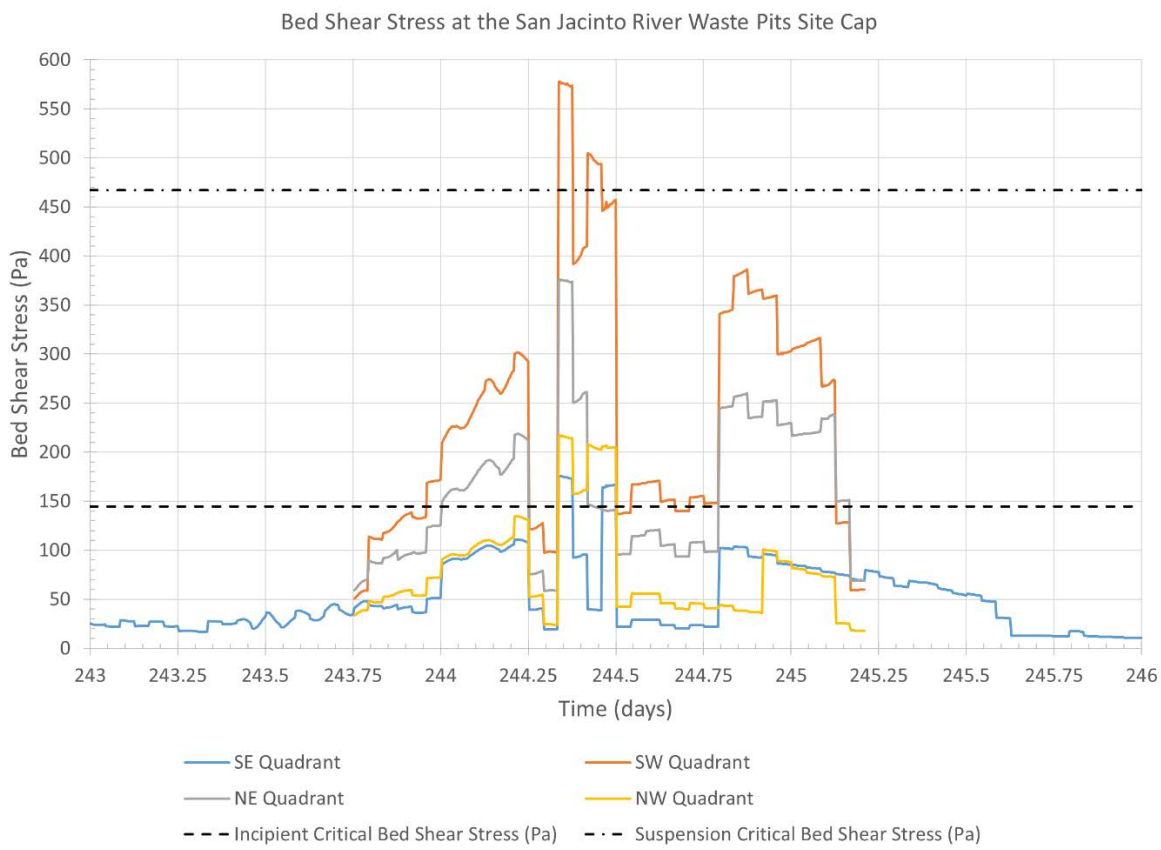

Figure 5-2 Calculated current- and wave-induced bed shear stress in all four quadrants of the San Jacinto Waste Pits cap

References

Ackers, P. and W.R. White. 1973. Sediment transport: a new approach and analysis. *Journal of Hydraulic Engineering*, 99 (HY11).

Anchor QEA. 2012. "Chemical Fate and Transport Modeling Study San Jacinto River Waste Pits Superfund Site," Ocean Springs, MS.

Anchor QEA. 2012. "Revised final removal action completion report San Jacinto River Waste Pits Superfund Site," Prepared for U.S. Environmental Protection Agency, Region 6, on behalf of McGinnes Industrial Maintenance Corporation and International Paper Company. http://galvbay.org/docs/SJRWP_Final_RACR_May%202012.pdf.

Anchor QEA. 2014. "Draft final interim feasibility study report San Jacinto River Waste Pits Superfund Site," Ocean Springs, MS.

Brody, S.D., R. Blessing, K. Atoba, W. Mobley, and M. Wilson. 2014. "A Flood Risk Assessment of the San Jacinto River Waste Pit Superfund Site," Center for Texas Beaches and Shores, Texas A&M University, Galveston, TX.

Demirbilek, Z., L. Lin, and A. Zundel. 2007. WABED model in the SMS: Part 2. Graphical interface. Coastal and Hydraulics Laboratory Engineering Technical Note ERDC/CHL CHETN-I-74. Vicksburg, MS: U.S. Army Engineer Research and Development Center.

Demirbilek, Z. and J.D. Rosati. 2011. Verification and validation of the Coastal Modeling System, Report 1: Summary Report, ERDC/CHL Technical Report 11-10, U.S. Army Corps of Engineers Research and Development Center, Vicksburg, MS.

Dyer, K.R. 1997. *Estuaries, A Physical Introduction*, 2nd Ed., John Wiley & Sons, New York.

Galperin, B., L.H. Kantha, S. Hassid, and A. Rosati. 1988. A quasi-equilibrium turbulent energy model for geophysical flows. *J. Atmos. Sci.,* **45**, 55-62.

Hamrick, J.M. 2007a. The Environmental Fluid Dynamics Code User Manual: US EPA Version 1.01. Tetra Tech, Inc., Fairfax, VA.

Hamrick, J.M. 2007b. The Environmental Fluid Dynamics Code Theory and Computation. Volume 1: Hydrodynamics and Mass Transport. Tetra Tech, Inc., Fairfax, VA.

Hamrick, J.M. 2007c. The Environmental Fluid Dynamics Code Theory and Computation. Volume 2: Sediment and Contaminant Transport and Fate. Tetra Tech, Inc., Fairfax, VA.

Hayter, E., J. Smith, D. Michalsen, Z. Demirbilek, and L. Lin. 2012. Dredged Material Placement Site Capacity Analysis for Navigation Improvement Project at Grays Harbor, WA. *ERDC/CHL Technical Report TR-08-13*. U.S. Army Engineer Research and Development Center, Vicksburg, MS,

Lin, L., Z. Demirbilek, and F. Yamada. 2008. CMS-Wave: A nearshore spectral wave processes model for coastal inlets and navigation projects. Coastal and Hydraulics Laboratory Technical Report ERDC/CHL TR-08-13. Vicksburg, MS: U.S. Army Engineer Research and Development Center.

Lin, L., Z. Demirbilek, and H. Mase. 2011a. Recent capabilities of CMS-Wave: A coastal wave model for inlets and navigation projects. Proceedings, Symposium to honor Dr. Nicholas Kraus. *Journal of Coastal Research*, Special Issue 59, 7-14.

Lin, L., Z. Demirbilek, R. Thomas, and J. Rosati. 2011b. Verification and validation of the Coastal Modeling System, Report 2: CMS-Wave, ERDC/CHL Technical Report 11-10, U.S. Army Corps of Engineers Research and Development Center, Vicksburg, MS.

USGS. 1995. "Floods in Southeast Texas, October 1994," U.S. Geological Survey, Houston, TX.

Zundel, A.K. 2006. Surface-water modeling system reference manual – Version 9.2. Provo, UT: Brigham Young University Environmental Modeling Research Laboratory.

Appendix A

Description of LTFATE Modeling System

LTFATE is a multi-dimensional modeling system maintained by ERDC (Hayter *et al*. 2012). The hydrodynamic module in LTFATE is the Environmental Fluid Dynamics Code (EFDC) surface water modeling system (Hamrick 2007a; 2007b; and 2007c). EFDC is a public domain, three-dimensional finite difference model that contains dynamically linked hydrodynamic and sediment transport modules. Brief descriptions of these two modules are described below.

Hydrodynamic module in LTFATE

EFDC can simulate barotropic and baroclinic flow in a water body due to astronomical tides, wind, density gradients, and river inflow. It solves the three-dimensional (3D), vertically hydrostatic, free surface, turbulence averaged equations of motion. EFDC is extremely versatile, and can be used for 1D, 2D-laterally averaged (*2DV*), 2D-vertically averaged (2DH), or 3D simulations of rivers, lakes, reservoirs, estuaries, coastal seas, and wetlands.

For realistic representation of horizontal boundaries, the governing equations in EFDC are formulated such that the horizontal coordinates, x and y, are curvilinear. To provide uniform resolution in the vertical direction, the sigma (stretching) transformation is used. The equations of motion and transport solved in EFDC are turbulence-averaged, because prior to averaging, although they represent a closed set of instantaneous velocities and concentrations, they cannot be solved for turbulent flows. A statistical approach is applied, where the instantaneous values are decomposed into mean and fluctuating values to enable the solution. Additional terms that represent turbulence are introduced to the equations for the mean flow. Turbulent equations of motion are formulated to utilize the Boussinesq approximation for variable density. The Boussinesq approximation accounts for variations in density only in the gravity term. This assumption simplifies the governing equations significantly, but may introduce large errors when density gradients are large.

The resulting governing equations, presented in Appendix B, include parameterized, Reynolds-averaged stress and flux terms that account for the turbulent diffusion of momentum, heat and salt. The turbulence parameterization in EFDC is based on the Mellor and Yamada (1982) level 2.5 turbulence closure scheme, as modified by Galperin *et al.* (1988) that relates turbulent correlation terms to the mean state variables. The EFDC model also solves several transport and transformation equations for different dissolved and suspended constituents, including suspended sediments, toxic contaminants, and water quality state variables. Detailed descriptions of the model formulation and numerical solution technique used in EFDC are provided by Hamrick (2007b). Additional capabilities of EFDC include: 1) simulation of wetting and drying of flood plains, mud flats, and tidal marshes; 2) integrated, near-field mixing zone model; 3) simulation of hydraulic control structures such as dams and culverts; and 4) simulation of wave boundary layers and wave-induced mean currents. A more detailed description of EFDC is given in Appendix B.

Sediment transport module

The sediment transport model in LTFATE is a modified version of the SEDZLJ mixed sediment transport model (Jones and Lick 2001; James *et al.* 2010) that a) includes a three-dimensional representation of the sediment bed, and b) can simulate winnowing and armoring of the surficial layer of the sediment bed. SEDZLJ is dynamically linked to LTFATE in that the hydrodynamics and sediment transport modules are both run during each model time step. This enables simulated changes in morphology to be instantly fed-back to the hydrodynamic model. A more detailed description of SEDZLJ is given in Appendix C.

One of the first steps in performing sediment transport modeling is to use grain size distribution data from sediment samples collected at different locations throughout the model domain to determine how many discrete sediment size classes are needed to adequately represent the full range of sediment sizes. Typically, three to eight size classes are used. For example, AQ used four sediment size classes in their sediment transport model of the SJR. One size class was used to represent sediment in the cohesive sediment size range, 5 μm, and three size classes were used to represent the noncohesive sediment size range, 140, 510 and 3,500 μm.

Appendix B

Description of LTFATE Hydrodynamic Module

EFDC is a public domain, 3D finite difference model that contains dynamically linked hydrodynamic and sediment transport modules. EFDC can simulate barotropic and baroclinic flow in a water body due to astronomical tides, wind, density gradients, and river inflow. It solves the 3D vertically hydrostatic, free surface, turbulence averaged equations of motion. EFDC can be used for 1D, 2D-laterally averaged (*2DV*), 2D-vertically averaged (2DH), or 3D simulations of rivers, lakes, reservoirs, estuaries, coastal seas, and wetlands.

EFDC solves the 3D Reynolds-averaged equations of continuity (Equation B-1), linear momentum (Equations B-2 and B-3), hydrostatic pressure (Equation B-4), equation of state (Equation B-5) and transport equations for salinity and temperature (Equations B-6 and B-7) written for curvilinear-orthogonal horizontal coordinates and a sigma (stretching) vertical coordinate. These are given by Hamrick (2007b) and repeated below:

$$\frac{\partial(m\varepsilon)}{\partial t}+\frac{\partial(m_y Hu)}{\partial x}+\frac{\partial(m_x Hv)}{\partial y}+\frac{\partial(mw)}{\partial z}=0 \qquad \text{(B-1)}$$

$$\frac{\partial(mHu)}{\partial t}+\frac{\partial(m_y Huu)}{\partial x}+\frac{\partial(m_x Hvu)}{\partial y}+\frac{\partial(mwu)}{\partial z}-$$
$$(mf+v\frac{\partial(m_y)}{\partial x}-u\frac{\partial m_x}{\partial y})Hv=m_y H\frac{\partial(g\varepsilon+p)}{\partial x}- \qquad \text{(B-2)}$$
$$m_y(\frac{\partial H}{\partial x}-z\frac{\partial H}{\partial x})\frac{\partial p}{\partial z}+\frac{\partial(mH^{-1}A_v\frac{\partial u}{\partial z})}{\partial z}+Q_u$$

$$\frac{\partial(mHv)}{\partial t}+\frac{\partial(m_y Huv)}{\partial x}+\frac{\partial(m_x Hvv)}{\partial y}+\frac{\partial(mwv)}{\partial z}+$$
$$(mf+v\frac{\partial(m_y)}{\partial x}+u\frac{\partial m_x}{\partial y})Hu=m_x H\frac{\partial(g\varepsilon+p)}{\partial y}- \qquad \text{(B-3)}$$
$$m_x(\frac{\partial H}{\partial y}-z\frac{\partial H}{\partial y})\frac{\partial p}{\partial z}+\frac{\partial(mH^{-1}A_v\frac{\partial v}{\partial z})}{\partial z}+Q_v$$

$$\frac{\partial p}{\partial z}=\frac{gH(\rho-\rho_o)}{\rho_o}=gHb \qquad \text{(B-4)}$$

$$\rho=\rho(\rho,S,T) \qquad \text{(B-5)}$$

$$\frac{\partial(mHS)}{\partial t}+\frac{\partial(m_y HuS)}{\partial x}+\frac{\partial(m_x HvS)}{\partial y}+\frac{\partial(mwS)}{\partial z}=\frac{\partial(\frac{mA_b}{H}\frac{\partial S}{\partial z})}{\partial z}+Q_s \qquad \text{(B-6)}$$

$$\frac{\partial(mHT)}{\partial t}+\frac{\partial(m_y HuT)}{\partial x}+\frac{\partial(m_x HvT)}{\partial y}+\frac{\partial(mwT)}{\partial z}=\frac{\partial(\frac{mA_b}{H}\frac{\partial T}{\partial z})}{\partial z}+Q_T \qquad \text{(B-7)}$$

where u and v are the mean horizontal velocity components in (x,y) coordinates; m_x and m_y are the square roots of the diagonal components of the metric tensor, and $m = m_x m_y$ is the Jacobian or square root of the metric tensor determinant; p is the pressure in excess of the reference pressure, $\frac{\rho_o gH(1-z)}{\rho_o}$, where ρ_o is the reference density; f is the Coriolis parameter for latitudinal variation; A_v is the vertical turbulent viscosity; and A_b is the vertical turbulent diffusivity. The buoyancy b in Equation B-4 is the normalized deviation of density from the reference value. Equation B-5 is the equation of state that calculates water density, ρ, as functions of p, salinity, S, and temperature, T.

The sigma (stretching) transformation and mapping of the vertical coordinate is given as:

$$z=\frac{(z^*+h)}{(\xi+h)} \qquad \text{(B-8)}$$

where z^* is the physical vertical coordinate, and h and ξ are the depth below and the displacement about the undisturbed physical vertical coordinate origin, $z^* = 0$, respectively, and $H=h+\xi$ is the total depth. The vertical velocity in z coordinates, w, is related to the physical vertical velocity w^* by:

$$w = w^* - z\left(\frac{\partial \xi}{\partial t} + \frac{u}{m_x}\frac{\partial \xi}{\partial x} + \frac{v}{m_y}\frac{\partial \xi}{\partial y}\right) + (1 - z)\left(\frac{u}{m_x}\frac{\partial h}{\partial x} + \frac{v}{m_y}\frac{\partial h}{\partial y}\right) \qquad \text{(B-9)}$$

The solutions of Equations B-2, B-3, B-6 and B-7 require the values for the vertical turbulent viscosity and diffusivity and the source and sink terms. The vertical eddy viscosity and diffusivity, A_v and A_b, are parameterized according to the level 2.5 (second-order) turbulence closure model of Mellor and Yamada (1982), as modified by Galperin *et al.* (1988), in which the vertical eddy viscosities are calculated based on the turbulent kinetic energy and the turbulent macroscale equations. The Mellor and Yamada level 2.5 (MY2.5) turbulence closure model is derived by starting from the Reynolds stress and turbulent heat flux equations under the assumption of a nearly isotropic environment, where the Reynolds stress is generated due to the exchange of momentum in the turbulent mixing process. To make the turbulence equations closed, all empirical constants are obtained by assuming that turbulent heat production is primarily balanced by turbulent dissipation.

The vertical turbulent viscosity and diffusivity are related to the turbulent intensity, q^2, turbulent length scale, l and a Richardson number R_q as follows:

$$A_v = \Phi_v ql = 0.4(1 + 36R_q)^{-1}(1 + 6R_q)^{-1}(1 + 8R_q)ql \qquad \text{(B-10)}$$

$$A_b = \Phi_b ql = 0.5(1 + 36R_q)^{-1}ql \qquad \text{(B-11)}$$

where A_v and A_b are stability functions that account for reduced and enhanced vertical mixing or transport in stable and unstable vertical, density-stratified environments, respectively, and the local Richardson number is given as:

$$R_q = \frac{gH\frac{\partial b}{\partial z}}{q^2}\frac{l^2}{H^2} \qquad \text{(B-12)}$$

A critical Richardson number, R_q = 0.20, was found at which turbulence and mixing cease to exist (Mellor and Yamada 1982). Galperin *et al.* (1988) introduced a length scale limitation in the MY scheme by imposing an upper limit for the mixing length to account for the limitation of the vertical turbulent excursions in stably stratified flows. They also modified and introduced stability functions that account for reduced or enhanced vertical mixing for different stratification regimes.

The turbulence intensity (q^2) and the turbulence length scale (l) are computed using the following two transport equations:

$$\frac{\partial(mHq^2)}{\partial t} + \frac{\partial(m_y Huq^2)}{\partial x} + \frac{\partial(m_x Hvq^2)}{\partial y} + \frac{\partial(mwq^2)}{\partial z} = \frac{\partial\left(\frac{mA_q \frac{\partial q^2}{\partial z}}{H}\right)}{\partial z} + Q_q \quad \text{(B-13)}$$
$$+ 2\frac{mA_v}{H}\left(\left(\frac{\partial^2 u}{\partial z^2}\right) + \left(\frac{\partial^2 v}{\partial z^2}\right)\right) + 2mgA_b\frac{\partial b}{\partial z} - 2mH\left(\frac{q^3}{(B_1 l)}\right)$$

$$\frac{\partial(mHq^2 l)}{\partial t} + \frac{\partial(m_y Huq^2 l)}{\partial x} + \frac{\partial(m_x Hvq^2 l)}{\partial y} + \frac{\partial(mwq^2 l)}{\partial z} =$$
$$\frac{\partial\left(\frac{mA_q \frac{\partial q^2 l}{\partial z}}{H}\right)}{\partial z} + Q_l + 2\frac{mE_1 lA_v}{H}\left(\left(\frac{\partial^2 u}{\partial z^2}\right) + \left(\frac{\partial^2 v}{\partial z^2}\right)\right) + mgE_1E_3 lA_b\frac{\partial b}{\partial z} \quad \text{(B-14)}$$
$$- H\left(\frac{q^3}{(B_1)}\right)(1 + E_2(\kappa L)^{-2} l^2)$$

The above two equations include a wall proximity function, $W = 1 + E_2 l(\kappa L)^{-2}$, that assures a positive value of diffusion coefficient $L^{-1} = (H)^{-1}(z^{-1} + (1 - z)^{-1})$). κ, B_1, E_1, E_2, and E_3 are empirical constants with values 0.4, 16.6, 1.8, 1.33, and 0.25, respectively. All terms with *Q's* (Q_u, Q_v, Q_q, Q_l, Q_s, Q_T) are sub-grid scale sink-source terms that are modeled as sub-grid scale horizontal diffusion. The vertical diffusivity, A_q, is in general taken to be equal to the vertical turbulent viscosity, A_v (Hamrick 2007b).

The vertical boundary conditions for the solutions of the momentum equations are based on the specification of the kinematic shear stresses. At

the bottom, the bed shear stresses are computed using the near bed velocity components (u_1,v_1) as:

$$(\tau_{bx}, \tau_{by}) = c_b \sqrt{u_1^2 + v_1^2}(u_1, v_1) \qquad \text{(B-15)}$$

where the bottom drag coefficient $c_b = (\frac{\kappa}{\ln(\Delta_1/2z_o)})^2$, where κ is the von Karman constant, Δ_1 is the dimensionless thickness of the bottom layer, $z_o = z_o^*/H$ is the dimensionless roughness height, and z_o^* is roughness height in meters. At the surface layer, the shear stresses are computed using the u, v components of the wind velocity (u_w,v_w) above the water surface (usually measured at 10 m above the surface) and are given as:

$$(\tau_{sx}, \tau_{sy}) = c_s \sqrt{u_w^2 + v_w^2}(u_w, v_w) \qquad \text{(B-16)}$$

where $c_s = 0.001\frac{\rho_a}{\rho_w}(0.8 + 0.065\sqrt{u_w{}^2 + v_w^2})$ and ρ_a and ρ_w are the air and water densities, respectively. Zero flux vertical boundary conditions are used for the transport equations.

Numerically, EFDC is second-order accurate both in space and time. A staggered grid or C-grid provides the framework for the second-order accurate spatial finite differencing used to solve the equations of motion. Integration over time involves an internal-external mode splitting procedure separating the internal shear, or baroclinic mode, from the external free surface gravity wave, or barotropic mode. In the external mode, the model uses a semi-implicit scheme that allows the use of relatively large time steps. The internal equations are solved at the same time step as the external equations, and are implicit with respect to vertical diffusion. Details of the finite difference numerical schemes used in the EFDC model are given in Hamrick (2007b), and will not be presented in this report.

The generic transport equation solved in EFDC for a dissolved (*e.g.*, chemical contaminant) or suspended (*e.g.*, sediment) constituent having a mass per unit volume concentration C, is

$$\frac{\partial m_x m_y HC}{\partial t} + \frac{\partial m_y HuC}{\partial x} + \frac{\partial m_x HvC}{\partial y} + \frac{\partial m_x m_y wC}{\partial z} - \frac{\partial m_x m_y w_{sc} C}{\partial z} =$$
$$\frac{\partial}{\partial x}\left(\frac{m_y}{m_x} HK_H \frac{\partial C}{\partial x}\right) + \frac{\partial}{\partial y}\left(\frac{m_x}{m_y} HK_H \frac{\partial C}{\partial y}\right) + \frac{\partial}{\partial z}\left(m_x m_y \frac{K_v}{H} \frac{\partial C}{\partial z}\right) + Q_c \qquad \text{(B-17)}$$

where K_V and K_H are the vertical and horizontal turbulent diffusion coefficients, respectively; w_{sc} is a positive settling velocity when C represents the mass concentration of suspended sediment; and Q_c represents external sources or sinks and reactive internal sources or sinks. For sediment, $C = S_i$, where S_i represents the concentration of the *ith* sediment class. So, Eq. B-17, which is the 3D advective-dispersive transport equation, is solved for each of the sediment size classes that the grain size distribution at the site is divided into. In this case, Q_{ci} = source/sink term for the *ith* sediment size class that accounts for erosion/deposition. The equation used to calculate Q_{ci} is the following:

$$S_i = E_{sus,i} - D_{sus,i} \qquad \text{(B-18)}$$

where $E_{sus,i}$ = sediment erosion rate for the *ith* sediment size class that is eroded and entrained into suspension, and $D_{sus,i}$ = sediment deposition rate for the *ith* sediment size class. Expressions for $D_{sus,i}$ and $E_{sus,i}$ are given later in this chapter.

The solution procedure for Eq. B-17 is the same as that for the salinity and heat transport equations, which use a high-order upwind difference solution scheme for the advection terms (Hamrick 2007b). Although the advection scheme is designed to minimize numerical diffusion, a small amount of horizontal diffusion remains inherent in the numerical scheme. As such, the horizontal diffusion terms in Equation B-17 are omitted by setting K_H equal to zero.